

Electrostatic Actuation of AFM Cantilevers in Aqueous Solutions

Thomas Hackl, Mathias Poik and Georg Schitter *Senior Member, IEEE*,
Automation and Control Institute (ACIN)
Technische Universität Wien
Vienna, Austria
hackl@acin.tuwien.ac.at

Abstract—Performing electrical Atomic Force Microscopy measurements in aqueous solutions is of paramount importance in a vast range of scientific fields. As with operation at ambient conditions, it is important to ensure that the force on the cantilever is purely of electrostatic origin. However, with the insertion of water and therefore mobile ions and polar molecules into the tip-sample system come several unwanted effects. Here, an experimental study is carried out, analyzing the influence of parameters such as drive-frequency, -amplitude and ionic concentration on the feasibility to perform electrical AFM measurements in aqueous solutions. To this end the system is theoretically modelled and parameter sweeps are performed, leading to transition frequencies above which the electrostatic force has the predominant impact on the cantilever.

Index Terms—atomic force microscopy, electrostatic cantilever actuation, aqueous solution

I. INTRODUCTION

Atomic Force Microscopy (AFM) [1] has become a standard tool for the investigation of various processes at the nanoscale due to its high lateral resolution and sensitivity. In particular, electrical AFM measurements have gained importance in the recent years as they can deliver insight into very fundamental physical processes, ranging from corrosion [2] over biomolecular interaction [3] to energy conversion/storage [4]. Since most of these processes take place at the solid-liquid interface at an electrode, there is a need for further development of electrical AFM measurement modes regarding the fundamental differences between cantilever actuation in air and liquids [5].

There are several points which need to be considered, when moving from electric AFM measurements at ambient conditions to liquids. Firstly, the increased viscosity of the environment greatly influences the dynamic properties of the oscillating cantilever. Reduced resonance frequencies and quality factors are a result of the increased effective mass and damping, respectively [6]. Secondly, electrostatic actuation [7] or electric AFM modes (e.g. Kelvin-probe Force Microscopy KPFM [8], Scanning Capacitance Microscopy SCM [9], Piezoresponse Force Microscopy PFM [10]) require the application of an ac voltage to the cantilever and rely on defined conditions of the surrounding medium. However, in liquids the system between the cantilever and the sample is no

longer a loss-less homogeneous dielectric, uninfluenced by the measurement parameters such as electrical drive frequency and amplitude. Aqueous solutions in particular exhibit an electric dipole of the water molecules and are therefore subject to electric polarisation. This states a challenge and makes any AFM measurement, where external electric fields in the tip-sample system are involved, non-trivial [11]. Furthermore, the ever increasing field of AFM measurements in biological sciences demands operation in solutions with biologically relevant ionic concentrations (~ 100 mM/l). However, the presence of mobile ions poses additional complications on the dynamic behaviour of AFM cantilevers. Solvated ions move in response to an electric field and redistribute themselves, forming concentration gradients in the surroundings of the cantilever. The resultant osmotic pressure, trying to equilibrate the ion concentration, parasitically acts on the cantilever [12]. Together with other spurious effects, ranging from electrophoretic displacement of dispersed particles to electrochemically induced surface stress [13], a set of forces is formed disrupting any electric AFM measurement in liquids. There has been a great research effort to analyze and theoretically describe the different force contributions on cantilevers suspended in an ion containing liquid [12], [14]. However, a clear separation of electrostatic to other force contributions has yet to undergo a detailed experimental verification.

The contribution of this paper is to analyze the influence of an aqueous solution with a specific ionic concentration on the feasibility to electrostatically excite AFM cantilevers in liquids. Transition frequencies are quantified above which electrostatic forces become dominant over other parasitic force contributions, enabling electric AFM measurements. A comprehensive physical model including the involved forces is introduced in the next section. The experimental section consists of a set of bode plots, analyzing the influence of drive frequency and ionic concentration on the feasibility to perform electric AFM measurements in aqueous solutions. The last section deals with the influence of the tip-sample distance and closes with a discussion.

II. MODELLING OF ELECTROSTATIC CANTILEVER ACTUATION IN LIQUIDS

Applying an ac voltage between a sample and a cantilever suspended in an electrolyte solution, is necessary for several

The financial support by the Austrian Science Fund FWF (Project Nr. P 31238-N28) and the Austrian Research Promotion Agency FFG (Project Nr. 883916) is gratefully acknowledged.

electric AFM modes but comes with some unwanted effects. Due to the violation of the local charge neutrality (voltage on cantilever), solvated ions migrate towards the cantilever and the sample (i.e. electromigration), forming an electric double layer (EDL) [15]. The formed concentration gradient away from the surface results in an osmotic pressure. Switching the polarity of the applied voltage repels the adhered ions and attracts ions of different charge. An ac voltage is therefore inducing an osmotic force component oscillating with the same frequency. However, as the mobility of the ions in the solution is limited by their concentration and diffusion constant, increasing the frequency leads to reduced ion mobility, eventually vanishing at very high frequencies. This parasitic force term F_p , acting on the electrically excited cantilever can therefore be modelled as a low-pass [16]:

$$F_p(f) = \frac{1}{1 + i\left(\frac{f}{f_p}\right)^\alpha} \cdot F_{p0} \cdot e^{i\phi_p}, \quad (1)$$

where $F_{p0} \cdot e^{i\phi_p}$ is a complex effective parasitic force at low-frequencies with a cut-off frequency f_p and a fitting parameter α . The electrostatic force is generally expressed as the derivation of the capacitively stored energy between the cantilever and the sample along their separation z :

$$F_{el} = \frac{\partial C \cdot U^2}{\partial z \cdot 2} = \frac{1}{2} \frac{\partial C}{\partial z} (\phi - U_C)^2, \quad (2)$$

where $\frac{\partial C}{\partial z}$ is the tip-sample capacitance gradient, ϕ the sample surface potential and U_C the applied voltage. Together, these forces act on the cantilever, which is usually modelled as a damped harmonic oscillator model [14] given by the transfer function:

$$G(f) = \frac{Q}{Q \left[1 - \left(\frac{f}{f_1}\right)^2 \right] + i\left(\frac{f}{f_1}\right)} \cdot \frac{1}{k}, \quad (3)$$

where f_1 is the first flexural resonance frequency, k the stiffness and Q the quality factor (at f_1) of the oscillating cantilever. The separation of the individual force contributions is challenging, as an excitation with the voltage $a \cdot \sin(\omega t)$ leads to an undefined combination of parasitic and electrostatic forces. Therefore, the voltage $U_C = a \cdot \sin(\omega t) + b \cdot \cos(2\omega t)$ is applied to the cantilever in the following. This has the reason, that the resultant electrostatic force components oscillating with ω and 2ω can be separated from the parasitic components, which becomes more evident in the experimental section. The electrostatic force components oscillating with ω and 2ω , as a result of inserting U_C into Eqn. (2) are as follows:

$$\begin{aligned} F_{el,\omega} &= \frac{1}{2} \frac{\partial C}{\partial z} (2\phi a + ab) \cdot \sin(\omega t), \\ F_{el,2\omega} &= \frac{1}{2} \frac{\partial C}{\partial z} \left(2\phi b + \frac{a^2}{2} \right) \cdot \cos(2\omega t) \end{aligned} \quad (4)$$

In order to provide defined experimental conditions, the tip-sample distance is held constant at $20\mu\text{m}$ throughout all measurements. This ensures complete EDL charge screening of a possible surface potential ($\rightarrow \phi = 0$) [17], regardless of

the used ionic concentration. The resultant cantilever deflection amplitudes at ω and 2ω are therefore governed by following equations:

$$\begin{aligned} A_\omega &= G \left[F_{p,\omega} + \frac{1}{2} \frac{\partial C}{\partial z} (ab) \right] \\ A_{2\omega} &= G \left[F_{p,2\omega} + \frac{1}{2} \frac{\partial C}{\partial z} \left(\frac{a^2}{2} \right) \right]. \end{aligned} \quad (5)$$

It is worth to note, that the herein presented model does not account for force contributions by electrochemical reactions or electrochemically induced surface stress, which might have different transfer functions than Eqn. (1). However, by selecting suitable cantilevers these effects can be suppressed which is explained in more detail in the following.

III. SETUP AND EXPERIMENTAL DETAILS

The system to measure the transfer function of the electrostatically excited cantilever in liquids is illustrated in Figure 1. As discussed in the previous section, an ac voltage with two frequency components ($\omega, 2\omega$) is applied to the conducting cantilever. The resulting cantilever deflection is measured by the OBD method [18] and fed to a lock-in amplifier for demodulation. The lock-in reference is supplied by either the ω or 2ω signal to measure the oscillation amplitudes given by Eqn. (5). The demodulated amplitudes ($R_\omega, R_{2\omega}$) together with the phases ($\phi_\omega, \phi_{2\omega}$) are recorded as a function of drive frequency ω for different measurement conditions.

A commercial AFM (Multimode 8, Bruker, USA) with an external signal generator (33522B, Keysight Technologies, USA), an external lock-in amplifier (7270, Ametek, USA) and a DAQ card for data acquisition (6211, National Instruments, USA) are used for the measurements of the cantilever transfer

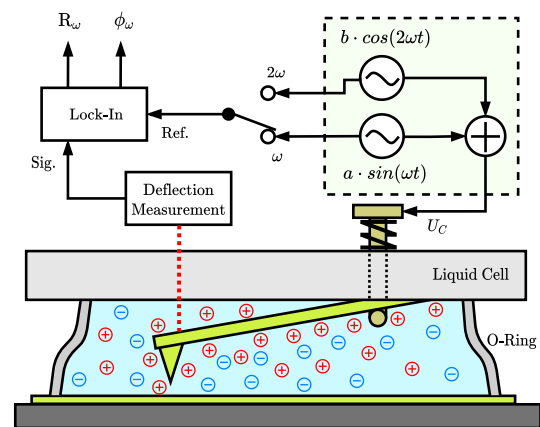


Fig. 1: System for electrostatically actuated cantilever transfer function measurements in liquids. A signal generator (dashed box) is used to supply the ac voltage U_C between the gold coated cantilever and sample and to provide the reference frequencies ($\omega, 2\omega$) to the lock-in amplifier, which demodulates the measured cantilever deflection.

function. A liquid cell (MTFML, Bruker, USA) is used to hold the overall gold coated cantilever (TAP300GB-G, Budget-Sensors, Bulgaria) (nominal stiffness: $k = 40 \text{ N/m}$) in place and to provide electrical connection. Using cantilevers with the same material on its top and bottom side minimizes the effect of electrochemically induced surface stress [13]. As sample a gold covered silicon substrate is glued onto an AFM specimen disc, using conductive silver paint (Micro-To-Nano, Netherlands). Chemically inert coatings on the sample and cantilever are used in order to prohibit parasitic electrochemical reactions (e.g. redox reactions). An s-shaped o-ring is used to prevent leakage of the measurement solution, which is supplied to the cell via an in- and outlet on the side of the liquid cell. Solutions of 1 mM and 10 mM ionic concentration are prepared, by diluting a 100 mM sodium chloride (NaCl) solution (AVS titrinorm, VWR chemicals, USA) with highly deionized water (milli-Q water, Millipore, USA) in a 1:10 ratio. After placing the sample and the liquid cell with the cantilever into the AFM, the measurement solution is inserted via a syringe connected to the inlet port of the cell. The laser is aligned onto the cantilever for deflection read-out and the cantilever is positioned $20 \mu\text{m}$ above the sample. Exchanging the measurement solution is done, by thorough flushing the liquid cell with deionized water, subsequent drying and inlet of the new solution.

IV. INFLUENCE OF MEASUREMENT PARAMETERS ON ELECTROSTATIC CANTILEVER ACTUATION

A. Ionic Concentration

Figure 2 shows a bode plot of an electrostatically actuated cantilever in various media. Drive amplitudes of $a = 2 \text{ V}$ and $b = 2 \text{ V}$ are chosen to achieve a reasonable signal-to-noise ratio (SNR). The measurement in air shows a resonance at 224.8 kHz and a flat response for low frequencies. In deionized water, the resonance is reduced to 110.2 kHz with the same behaviour at low frequencies. Fitting the cantilever model (Eqn. (5)) to the observed transfer functions, leads to following resonance frequencies and Q factors:

	Air	DI
resonance frequency: f_1 (kHz)	224.8	110.2
quality factor: Q	307	8.5

TABLE I: Resonance frequency and quality factor of electrostatically actuated cantilever in air and deionized water.

The increased damping in water reduces the resonance frequency and Q-factor by a factor of ~ 2 and ~ 36 , respectively. As the ionic concentration increases the transfer function further deviates from its initial form, especially at low frequencies, which corresponds to the introduced theoretical description. The dashed lines represent fitted transfer functions according to the parameters in the figures caption. From these measurements it emanates, that a frequency boundary between the parasitic and electrostatic force contributions exist, which shifts to higher frequencies with increasing molarity. In the

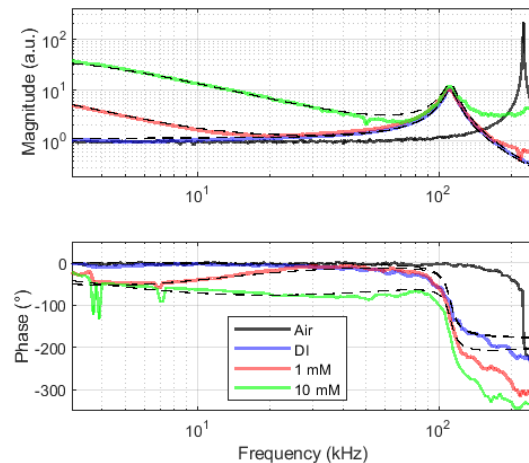


Fig. 2: Bode Plot of an electrostatically excited cantilever in air and aqueous solution of varying ionic concentration. The dashed lines represent fitted models based on Eqn. (5) with following fitting parameters: $\alpha = 1.2$, $\phi_p = 5^\circ$, $F_{es} = 45$ | DI: $F_{p0} = 0$ | 1mM: $F_{p0} = 450$, $f_p = 1.5$ | 10mM: $F_{p0} = 1680$, $f_p = 3.5$ [14].

following, the individual force contributions are changed by sweeping the drive amplitudes a and b in order to quantify this transition frequency.

B. Electrical drive amplitudes: a , b

Figure 3 (a,b) shows bode plots in a 1 mM sodium chloride solution for different drive amplitudes a (a) and b (b), when locking on the frequency ω . For frequencies higher than $\sim 10 \text{ kHz}$ a linear dependence of R_ω on the drive amplitudes, as described by Eqn. (5) is observed. At low frequencies however, this connection is violated, as a variation of b shows only a minor influence on the cantilever deflection amplitude. The same effect is observed, when switching the lock-in reference frequency to 2ω (Fig. 3 (c,d)). Above a certain frequency, the cantilever deflection magnitude follows accurately Eqn. (5) (quadratic dependence on a and no influence of b). At low frequencies however, the effect is inverted. The deflection amplitude is mainly determined by the choice of b and shows almost now dependence on the drive amplitude a .

The observed behaviour further underpins the theory of induced ionic motion in the solution, as the magnitudes of R_ω and $R_{2\omega}$ at low frequencies are mainly caused by the drive signals of their respective lock-in reference frequencies. i.e. An oscillating electric field induces ionic motion and therefore parasitic forces only at the same frequency. Quantifying the transition frequency between domains where parasitic and electrostatic forces dominate is possible by relating the measured amplitude responses to each other, which is done in the following.

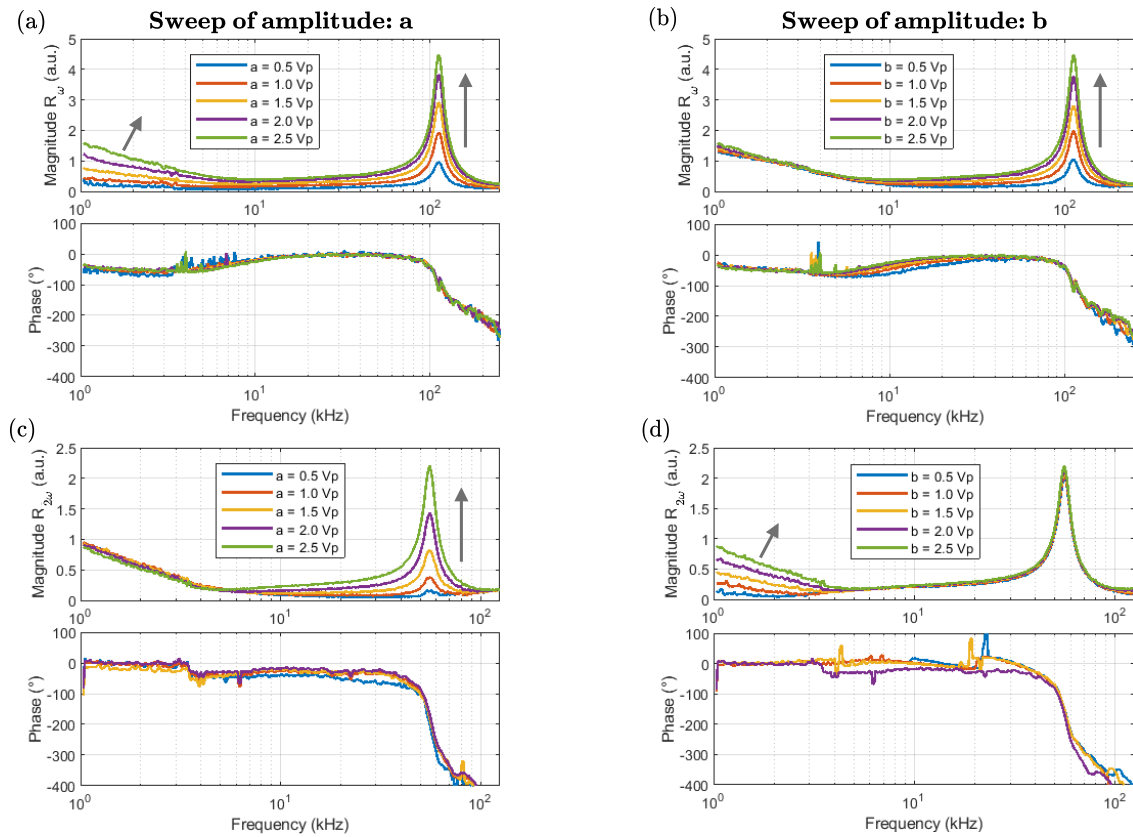


Fig. 3: (a,b) Bode plot of electrostatically actuated cantilever for different drive amplitudes a ($b = 2.5V$) (a) and b ($a = 2.5V$) (b) for a lock-in reference frequency of ω . (c,d) shows the same plot for a lock-in reference frequency of 2ω , which results in the resonance appearing at $f_1/2$. Ionic concentration: 1 mM / tip-sample separation: 20 μm (arrows denote direction of increased drive amplitude).

C. Transition of parasitic to electrostatic actuation

Figure 4 visualizes the transition of dominant parasitic to dominant electrostatic cantilever actuation for various ionic concentrations. The curves are computed by dividing the measured amplitude responses R_ω (Fig. 3(a)) at drive amplitudes a & b of 2 & 2.5 Vp by the ones of 1 & 2.5 Vp, respectively. For pure electrostatic excitation ($F_{p,\omega} = 0$) the deflection amplitude should double as given by Eqn. (5), which corresponds to an expected value of 2. However, it can be observed that below a certain frequency this statement does not hold true, indicating a dominant parasitic force contribution. The described computation is repeated for each individual curve of Fig. 3, leading to a comparable result. However, only one curve per ionic concentration is shown for clarity.

The curves settle to the expected value and therefore predominant electrostatic excitation above a frequency, which strongly depends on the molarity of the solution. This transition frequencies are determined to be 4.5 kHz, 24 kHz and 125 kHz for deionized water, 1 mM and 10 mM NaCl solution for a tip-

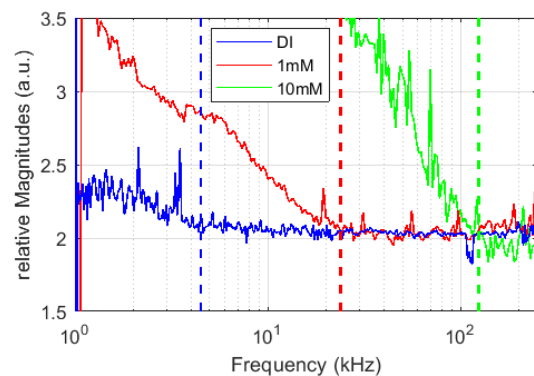


Fig. 4: Relation of individual amplitude responses of Fig. 3 as described in the text. The dashed lines represent the transition of dominant parasitic (left) to dominant electrostatic (right) cantilever actuation for the respective ionic concentration.

sample separation of 20 μm , respectively. It follows, that liquid AFM measurements involving the application of a voltage to the cantilever are only feasible in a regime where electrostatic forces dominate over parasitic contributions, which holds true for excitation frequencies above the transition frequency. A further interesting aspect is the influence of the tip-sample separation on the individual force contributions, which is discussed in the following.

D. Lift height

Figure 5 shows the normalized deflection amplitudes R_w for two different excitation frequencies ω (5 kHz and 110 kHz, $a = 2V$, $b = 2V$) as a function of lift-height in a 1 mM NaCl solution. A clear exponential distance dependence is observed for the high frequency excitation, which is usual for an electrostatic force. However, the low frequency excitation results in a mostly lift-height independent deflection amplitude, indicating parasitic origin due to ion mobility. Only below a lift-height of ~ 150 nm R_w significantly begins to rise, which can be explained by changing proportions of the individual force contributions ($\partial C/\partial z$ and therefore F_{el} rises whereas F_p stays constant with decreasing lift-height - Eqn. (5)). Thus, the observed result further underpins the validity of the theoretical description.

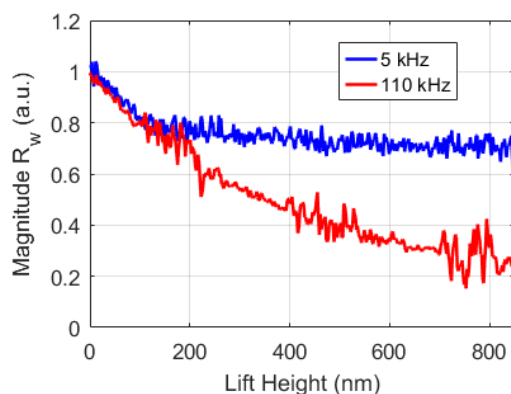


Fig. 5: Cantilever deflection as a function of lift height for two different excitation frequencies ω . A low frequency excitation (blue) results in a mostly lift-height uninfluenced deflection magnitude, indicating non-electrostatic (parasitic) force origin.

In summary, the frequency of the applied voltage to the cantilever should be greater than a molarity-dependent transition frequency in order to guarantee dominant electrostatic forces on the cantilever. Only in this case, parasitic forces due to ion motion are suppressed and electric AFM measurements in aqueous solutions are enabled.

V. CONCLUSION

A detailed experimental analysis of electrically driven AFM cantilevers in liquids of varying ionic concentration is carried out. The influence of ionic concentration and electric drive

frequency on the feasibility to perform electric AFM modes in aqueous solutions is analyzed. It is found that predominant electrostatic cantilever actuation, which is a prerequisite for electric AFM modes, is only possible above a certain excitation frequency, where parasitic force contributions due to ionic motion become recessive. This transition frequency is determined to be 4.5 kHz, 24 kHz and 125 kHz for deionized water, 1 mM and 10 mM sodium chloride solutions, respectively.

REFERENCES

- [1] G. Binnig, C. F. Quate, and C. Gerber, "Atomic force microscope," *Phys. Rev. Lett.*, vol. 56, pp. 930–933, Mar 1986.
- [2] M. Rohwerder and F. Turcu, "High-resolution kelvin probe microscopy in corrosion science: Scanning kelvin probe force microscopy (skpfm) versus classical scanning kelvin probe (skp)," *Electrochimica Acta*, vol. 53, no. 2, pp. 290–299, 2007.
- [3] A. K. Sinensky and A. M. Belcher, "Label-free and high-resolution protein/dna nanoarray analysis using kelvin probe force microscopy," *Nature nanotechnology*, vol. 2, no. 10, pp. 653–659, 2007.
- [4] S. V. Kalinin and N. Balke, "Local electrochemical functionality in energy storage materials and devices by scanning probe microscopies: status and perspectives," vol. 22, no. 35, 1 2010.
- [5] T. E. Schäffer, J. P. Cleveland, F. Ohnesorge, D. A. Walters, and P. K. Hansma, "Studies of vibrating atomic force microscope cantilevers in liquid," *Journal of Applied Physics*, vol. 80, no. 7, pp. 3622–3627, 1996.
- [6] G. Y. Chen, R. J. Warmack, T. Thundat, D. P. Allison, and A. Huang, "Resonance response of scanning force microscopy cantilevers," *Review of Scientific Instruments*, vol. 65, no. 8, pp. 2532–2537, 1994.
- [7] K.-i. Umeda, K. Kobayashi, K. Matsushige, and H. Yamada, "Direct actuation of cantilever in aqueous solutions by electrostatic force using high-frequency electric fields," *Applied Physics Letters*, vol. 101, no. 12, p. 123112, 2012.
- [8] M. Nonnenmacher, M. P. O'Boyle, and H. K. Wickramasinghe, "Kelvin probe force microscopy," *Applied Physics Letters*, vol. 58, no. 25, pp. 2921–2923, 1991.
- [9] Y. Huang, C. C. Williams, and J. Slinkman, "Quantitative two-dimensional dopant profile measurement and inverse modeling by scanning capacitance microscopy," *Applied Physics Letters*, vol. 66, no. 3, pp. 344–346, 1995.
- [10] E. Soergel, "Piezoresponse force microscopy (PFM)," *Journal of Physics D: Applied Physics*, vol. 44, no. 46, p. 464003, nov 2011.
- [11] L. Collins, S. Jesse, J. I. Kilpatrick, A. Tselev, M. B. Okatan, S. V. Kalinin, and B. J. Rodriguez, "Kelvin probe force microscopy in liquid using electrochemical force microscopy," *Beilstein journal of nanotechnology*, vol. 6, pp. 201–214, 2015.
- [12] M. Checa, R. Millan-Solsona, and G. Gomila, "Frequency-dependent force between ac-voltage-biased plates in electrolyte solutions," *Physical review E*, vol. 100, no. 2-1, p. 022604, 2019.
- [13] R. Raiteri and H.-J. Butt, "Measuring electrochemically induced surface stress with an atomic force microscope," *The Journal of Physical Chemistry*, vol. 99, pp. 15 728–15 732, 1995.
- [14] K.-i. Umeda, K. Kobayashi, N. Oyabu, Y. Hirata, K. Matsushige, and H. Yamada, "Practical aspects of kelvin-probe force microscopy at solid/liquid interfaces in various liquid media," *Journal of Applied Physics*, vol. 116, no. 13, p. 134307, 2014.
- [15] Z. J. Han, R. Morrow, B. K. Tay, and D. McKenzie, "Time-dependent electrical double layer with blocking electrode," *Applied Physics Letters*, vol. 94, no. 4, p. 043118, 2009.
- [16] K.-i. Umeda, K. Kobayashi, N. Oyabu, Y. Hirata, K. Matsushige, and H. Yamada, "Analysis of capacitive force acting on a cantilever tip at solid/liquid interfaces," *Journal of Applied Physics*, vol. 113, no. 15, p. 154311, 2013.
- [17] K. Hirata, T. Kitagawa, K. Miyazawa, T. Okamoto, A. Fukunaga, C. Takatoh, and T. Fukuma, "Visualizing charges accumulated in an electric double layer by three-dimensional open-loop electric potential microscopy," *Nanoscale*, vol. 10, no. 30, pp. 14 736–14 746, 2018.
- [18] G. Meyer and N. M. Amer, "Novel optical approach to atomic force microscopy," *Applied Physics Letters*, vol. 53, no. 12, pp. 1045–1047, 1988.